

## Article

# Silver Nanoparticles Loaded on Polyethylene Terephthalate Films Grafted with Chitosan

Guadalupe Gabriel Flores-Rojas <sup>1</sup>, Felipe López-Saucedo <sup>2</sup>, Ricardo Vera-Graziano <sup>3</sup>, Héctor Magaña <sup>4</sup>,  
Eduardo Mendizábal <sup>1,\*</sup> and Emilio Bucio <sup>2,\*</sup>

<sup>1</sup> Departamento de Química e Ingeniería Química, Centro Universitario de Ciencias Exactas e Ingenierías, Universidad de Guadalajara, Blvd. M. García Barragán # 1451, Guadalajara 44430, Jalisco, Mexico

<sup>2</sup> Departamento de Química de Radiaciones y Radioquímica, Instituto de Ciencias Nucleares, Universidad Nacional Autónoma de México, Circuito Exterior, Ciudad Universitaria, Mexico City 04510, Mexico

<sup>3</sup> Instituto de Investigaciones en Materiales, Universidad Nacional Autónoma de México, Circuito Exterior, Ciudad Universitaria, Mexico City 04510, Mexico

<sup>4</sup> Facultad de Ciencias Químicas e Ingeniería, Universidad Autónoma de Baja California, Calzada Universidad # 14418, Parque Industrial Internacional Tijuana, Tijuana 22390, Mexico

\* Correspondence: lalomendizabal@hotmail.com (E.M.); ebucio@nucleares.unam.mx (E.B.)

**Abstract:** Currently, polyethylene terephthalate (PET) is one of the most widely used polymeric materials in different sectors such as medicine, engineering, and food, among others, due to its benefits, including biocompatibility, mechanical resistance, and tolerance to chemicals and/or abrasion. However, despite all these excellent characteristics, it is not capable of preventing the proliferation of microorganisms on its surface. Therefore, providing this property to PET remains a difficult challenge. Fortunately, different strategies can be applied to remove microorganisms from the PET surface. In this work, the surface of the PET film was functionalized with amino groups and later with a dicarboxylic acid, allowing a grafting reaction with chitosan chains. Finally, the chitosan coating was loaded with silver nanoparticles with an average size of  $130 \pm 37$  nm, presenting these materials with an average cell viability of 80%. The characterization of these new PET-based materials showed considerable changes in surface morphology as well as increased surface hydrophilicity without significantly affecting their mechanical properties. In general, the implemented method can open an alternative pathway to design new PET-based materials due to its good cell viability with possible bacteriostatic activity due to the biocidal properties of silver nanoparticles and chitosan.

**Keywords:** chitosan; silver; nanoparticles; polyethylene terephthalate; graft; coating



**Citation:** Flores-Rojas, G.G.; López-Saucedo, F.; Vera-Graziano, R.; Magaña, H.; Mendizábal, E.; Bucio, E. Silver Nanoparticles Loaded on Polyethylene Terephthalate Films Grafted with Chitosan. *Polymers* **2023**, *15*, 125. <https://doi.org/10.3390/polym15010125>

Academic Editor: Luminita Marin

Received: 24 November 2022

Revised: 23 December 2022

Accepted: 23 December 2022

Published: 28 December 2022



**Copyright:** © 2022 by the authors. Licensee MDPI, Basel, Switzerland. This article is an open access article distributed under the terms and conditions of the Creative Commons Attribution (CC BY) license (<https://creativecommons.org/licenses/by/4.0/>).

## 1. Introduction

The presence and proliferation of microorganisms as biofilm [1] on polymeric materials for medical use and food containers can cause adverse effects on healthcare as well as for the stored food [2,3]. Therefore, polymeric materials capable of inhibiting the proliferation of microorganisms have gained great relevance. Therefore, it is necessary to develop more durable and efficient materials capable of inhibiting the proliferation not only of bacteria but also of fungi and even viruses [4] that can cause infections in open wounds, as well as avoiding the modification of the organoleptic properties of food and the production of secondary compounds that can be harmful to health [2,5,6].

One of the most widely used materials in food and medical device packaging is polyethylene terephthalate (PET) due to its excellent mechanical properties and chemical stability under several conditions [7], availability, and low production cost. Therefore, PET is an ideal candidate for its use as antibacterial surfaces [8]. Approaches to providing antimicrobial activity can be classified into two types: the first can be achieved by incorporating antimicrobial agents into the polymeric matrix, and the second by modifying the surface and coating it with antimicrobial agents [9,10]. The latter approach is one

of the most widely used since it significantly maintains the polymeric matrix's original properties. This approach can be carried out through different methodologies, such as using covalently bonded coatings, which make them more stable in different physical–chemical environments. Antimicrobial coatings can be polymers from a natural or synthetic origin, providing new properties to the original material such as stimulus-response [11], bacteriostatic effects [12], biocompatibility [13], or allowing the loading and stabilization of nanomaterials [14]. In this context, chitosan, which is a polymer of natural origin, has shown antimicrobial activity against different pathogenic microorganisms with a high mortality rate and low toxicity to humans in various studies, making this polymer suitable for different applications in food [15], drug-delivery [16,17], biomedical devices [18,19], and other chemistry fields [20]. Chitosan is also used to stabilize and load nanoparticles synthesized using different methods [21,22] and to add new functional properties to coated nanoparticles by using chitosan as a carrier, such as in magnetic drug delivery systems [23,24]. Moreover, some nanoparticles are capable of providing antimicrobial activity through the release of metallic ions that affect the integrity of microorganisms, causing their death, as is the case with silver nanoparticles [25].

Chitosan has been widely modified to meet various biological and medical needs due to its active functional groups. Chemical modification is the commonly used method because its amino groups can participate in chemical reactions such as alkylation, quaternization, and condensation reactions with aldehydes and ketones. The hydroxyl group also gives rise to hydrogen bonding and some reactions, such as *o*-acetylation, cross-linking, and grafting [26,27]. Currently, the condensation reaction between the amino group and the carboxyl group is mainly used to modify the chemical properties of chitosan, improving its effect on metal nanoparticles, and reducing its possible toxic effects [28–30].

Chitosan is used as a coating on different materials, such as polyethylene terephthalate (PET), which is a slightly polar material and lacks active functional groups, making the adhesion, coating, or covalent grafting of chitosan difficult. In this research work, the surface of PET films was modified to perform the covalent grafting of chitosan, providing a suitable surface for loading silver nanoparticles. Additionally, the grafted chitosan chains possibly provide a bacteriostatic effect and a sustainable release of silver ions capable of inhibiting the proliferation of microorganisms and increasing the cytocompatibility of the final material.

## 2. Materials and Methods

### 2.1. Materials

Silver nitrate (99.9%), chitosan (75–85% deacetylated; 50–190 kDa), itaconic acid (99%), acetic acid, sodium carbonate, hydrochloric acid, ethylenediamine, and polyethylene terephthalate (PET) films (200  $\mu\text{m}$  thickness; average molecular weight 18 kDa; 34.3% crystallinity) were purchased from Aldrich Chemical Co. (St. Louis, MO, USA). Ethanol and distilled water were acquired from Baker (Mexico City, Mexico).

### 2.2. Methods

#### 2.2.1. Aminolysis Reaction (PETN)

Three previously weighed PET films were placed in 10 mL of ethylenediamine at a temperature of 40 °C and reacted for different reaction times (0.5–4 h). Subsequently, the films were sonicated for 1 h and thoroughly washed with distilled water, removing the abraded surface of the film and residues from the reaction medium. Experiments were carried out in triplicate. The loss percentage was calculated according to the following equation (Equation (1)):

$$\text{Weight loss (\%)} = 100[(W_{\text{PET}} - W_{\text{PETN}})/W_{\text{PET}}] \quad (1)$$

where  $W_{\text{PET}}$  is the weight of the unmodified PET film and  $W_{\text{PETN}}$  is the weight of the film once it has undergone the aminolysis reaction.

The quantification of the amino groups present on the surface of the film was carried out by acid-base titration. Three aminolysis reaction (PETN) films were placed in 10 mL of a hydrochloric acid solution [0.02 M], keeping them constantly stirred for 24 h. Subsequently, the excess of hydrochloric acid was titrated with a sodium carbonate solution [0.001 M]. The number of amino groups was calculated according to the following equation (Equation (2)):

$$\text{Ethylenediamine modification (\%)} = 100[6.1(V_{\text{HCl}}C_{\text{HCl}} - 2V_{\text{T}}C_{\text{NaC}})/W_{\text{PETN}}] \quad (2)$$

where  $V_{\text{HCl}}$  and  $C_{\text{HCl}}$  are the volume and concentration of the hydrochloric acid solution,  $V_{\text{T}}$  is the volume of the titration and  $C_{\text{NaC}}$  is the concentration of the sodium carbonate solution and  $W_{\text{PETN}}$  is weight of the PETN film.

#### 2.2.2. Michael Addition Reaction (PETI)

Three previously weighed PETN films were made to react at reflux for 48 h in 10 mL of ethanol and an excess of itaconic acid (200 mg). Subsequently, the obtained films were exhaustively washed with distilled water. The incorporated itaconic acid was calculated according to the next equation (Equation (3))

$$\text{Itaconic acid modification (\%)} = 100[(W_{\text{PETN}} - W_{\text{PETI}})/W_{\text{PETN}}] \quad (3)$$

where  $W_{\text{PETN}}$  is the weight of the PETN film and  $W_{\text{PETI}}$  is the weight of the film after the Michael addition reaction.

#### 2.2.3. Chitosan Grafting (PETC)

Three previously weighed Michael addition reaction (PETI) films were placed in 10 mL of an aqueous solution of chitosan 1% (*w/v*) and 0.5% (*v/v*) acetic acid for 48 h at 25 °C. After this time, the films were removed from the solution and placed under vacuum at a temperature of 90 °C for 6 h. Finally, the obtained films (PETC) were exhaustively washed with distilled water and dried.

The percentage of chitosan graft on the surface of the film was calculated according to the following equation (Equation (4)):

$$\text{Chitosan graft (\%)} = 100[(W_{\text{PETI}} - W_{\text{PETC}})/W_{\text{PETI}}] \quad (4)$$

where  $W_{\text{PETI}}$  and  $W_{\text{PETC}}$  are the weight of the PETI and PETC films.

#### 2.2.4. Load of Silver Nanoparticles on PETC Film (PETCAg)

Three previously weighed PETC films were placed in 10 mL of an aqueous solution of silver nitrate with different concentrations (500, 1000, 3000, and 5000 ppm) for 72 h at 25 °C in the presence of sunlight. After the reaction time, the films were removed from the solution and thoroughly washed with distilled water and dried. The number of nanoparticles loaded on the PETCAg film was determined by film calcination using the weight difference of the residues yield at 800 °C (Equation (5)).

$$\text{Silver load (\%)} = C_{\text{PETCAg}} - C_{\text{PETC}} \quad (5)$$

where  $C_{\text{PETCAg}}$  and  $C_{\text{PETC}}$  are the residue percentage of the PETCAg and PETC films provided by the TGA instrument.

#### 2.2.5. Cell Viability Study

Cell viability tests were performed using a BALB/3T3 fibroblast line (mouse). These experiments were performed to assess the toxicity of the films in an *in vitro* model for potential biomedical applications. For the experiments, 25 mg of each type of film were cut and placed in 96-well plates containing 3000 cells (fibroblasts), with Dulbecco's modified Eagle's medium (DMEM), penicillin–streptomycin, gentamicin, and Fetal Bovine Serum (FBS); the films were in contact with the cell medium for 24 h in an incubator at 37 °C (5%

CO<sub>2</sub>). Subsequently, the films were removed from the cell medium, and MTT kit reagent (Roche, Switzerland) was added and incubated again for 4 h; later, they were solubilized and incubated for 12 h. The 96-well plates were plated in a Multiskan FC spectrophotometer, Thermo Fisher Scientific (Waltham, MA, USA); the absorbances from each film were read at a wavelength of 620 nm. Finally, cell activity (viability) was determined, making a comparison with control cells, using the following equation (Equation (6)), and the results obtained were statically analyzed by analysis of variance (ANOVA) using Fisher's comparison (Figures S1–S7, Tables S1–S4):

$$\text{Cytocompatibility (\%)} = 100(\text{Abs}_{\text{Sample}} / \text{Abs}_{\text{Control}}) \quad (6)$$

### 2.3. Instrumental

Kruss DSA 100 drop shape analyzer (Matthews, NC, USA) was used to measure the contact angle on the surface of films at time 1 min.

Fourier Transform Infrared Attenuated Total Reflection (FTIR ATR) of dry samples was analyzed using a Perkin–Elmer Spectrum 100 spectrometer (Norwalk, CT, USA) of 16 scans.

Scanning electron microscope (SEM) images were acquired by the Zeiss Evo LS15 instrument (Jena, Germany), and small pieces of 0.5 cm in length were cut and coated with gold and analyzed under a high vacuum.

Thermogravimetric analysis (TGA) data of the weight loss and decomposition of films were heated at a rate of 10 °C min<sup>−1</sup> and run from 20 to 800 °C under nitrogen flow at 100 cm<sup>3</sup>/min in a TGA instrument Q50 TA Instruments (New Castle, DE, USA).

Differential scanning calorimetry (DSC) runs were recorded under a nitrogen flow at 100 cm<sup>3</sup>/min using a DSC 2010 calorimeter (TA Instruments, New Castle, DE, USA) from 25 to 250 °C at a heating rate of 10 °C min<sup>−1</sup>.

Mechanical properties of the films were studied by applying a uniaxial tension test, as described in ASTM D1708. All tests were carried out on an INSTRON 1125 (Instron Inc., Norwood, MA, USA) universal tensile testing machine at a crosshead speed of 10 mm/min, and all experiments were carried out in triplicate.

## 3. Results and Discussions

### 3.1. Chitosan Grafting on PET Film

PET films were functionalized by aminolysis using ethylenediamine as a reagent and solvent. This reaction was studied at different times at a temperature of 40 °C. The results showed a weight loss of the PET film in the functionalization process with amino groups (Figure 1a). The weight loss increased with the reaction time. In the IR-ATR spectra (Figure 1b), the intensity bands of amines barely changed, where PETN-0.5 corresponds to the sample with the shorter time of reaction (30 min), while PETN-4 corresponds to the longer time of reaction (4 h). This result was confirmed in the acid-base titration (Table 1), since the increment in the number of amino groups on the film surface was small. When reaction times longer than 4 h were used, film disintegration occurred when the films were washed.

According to the results obtained at different reaction times and infrared studies, the modified films with a reaction time of 1 h were selected to continue with the next chemical activation step of the PET film, which presented an average amount of primary amino groups on the surface of 0.0078 mmol quantified by acid-base titration, with a percentage of the modification of the film with ethylenediamine by a weight of 1.25 ± 0.5%. The next activation step was carried out through the Michael addition reaction, between the amino groups present on the surface film and itaconic acid; this reaction was carried out in ethanol at reflux for 48 h. The resulting films were exhaustively washed with methanol and water, providing a weight-average surface modification of the 0.8 ± 0.2%. Subsequently, the obtained films were placed in 10 mL water at 5% acetic acid with 1% chitosan for 48 h to 25 °C. Finally, the films were removed from the chitosan solution and incubated at 90 °C for

6 h under vacuum, showing grafting of  $1.38 \pm 0.2\%$  according to the weight of the chitosan. Once the films were obtained, they were placed in a solution of silver nitrate (3000 ppm) in the presence of sunlight to promote the reduction in silver ions and nucleation of silver to nanoparticles (Figure 2), resulting in an average load of  $6.3 \pm 1.3\%$  by weight of silver nanoparticles concerning the matrix.

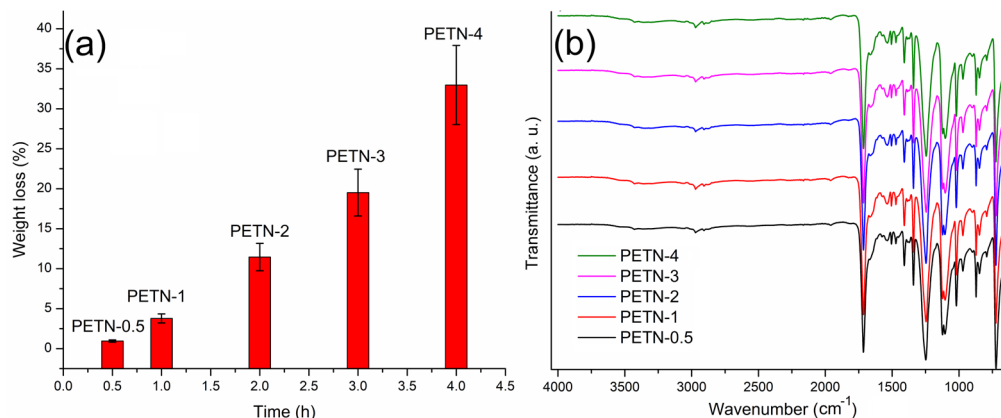


**Figure 1.** (a) Weight loss of PET films in the aminolysis reaction at different times, (b) IR-ATR spectra of PET films after aminolysis reaction at different times.

**Table 1.** Modification percentage of the PET film by the aminolysis reaction at different times, quantified by acid-base titration.

Time (h)	0.5	1	2	3	4
Modification PET with ethylenediamine (% w.)	$1.18 \pm 0.75$	$1.25 \pm 0.5$	$1.31 \pm 0.25$	$1.23 \pm 0.37$	$1.39 \pm 0.12$

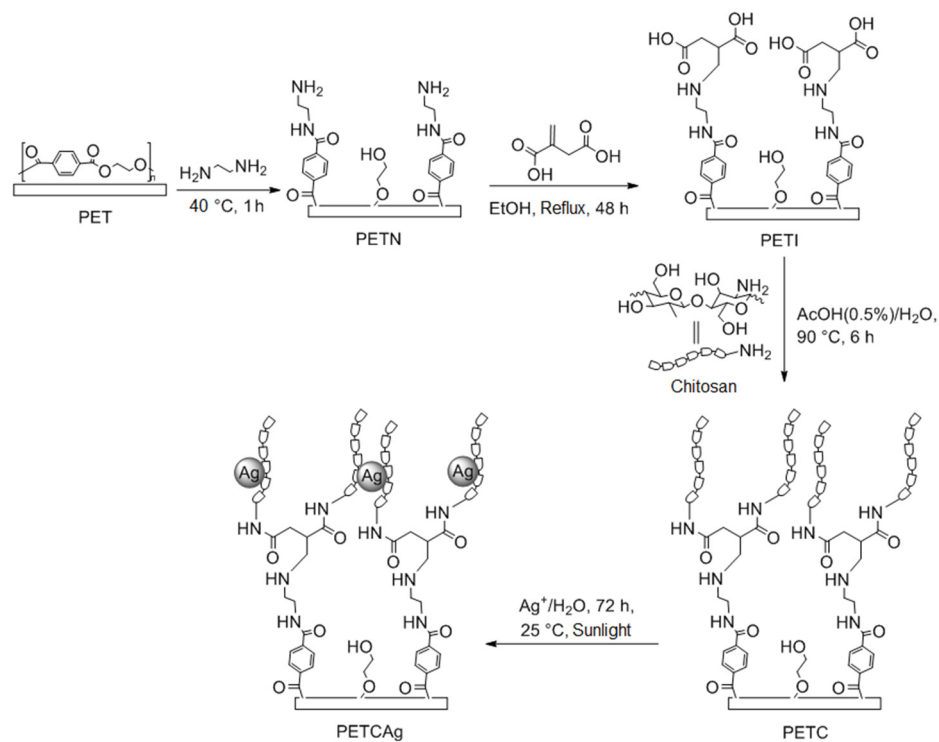


**Figure 2.** Scheme of chitosan graft on the functionalized PET film.

### 3.2. Contact Angle Study

Contact angle studies showed changes in the hydrophilicity of the films. The PET films had a contact angle of  $90^\circ$  which decreased to  $78^\circ$  when modified with ethylenediamine; moreover, upon reaction with itaconic acid, the angle slightly increased to  $88^\circ$ . These results are in accordance with the new hydrophilic groups present on the film surface. When grafting the chitosan chains, the contact angle increased to  $110^\circ$ . Finally, the loading of the silver nanoparticles caused a slight increase in the hydrophilicity of the film (Figure 3).



**Figure 3.** Contact angle of superficially modified films.

### 3.3. FTIR-ATR Analysis

TIR-ATR spectra (Figure 4a) were recorded to obtain information about the chemical groups incorporated into the PET films. The bands that evidenced the incorporation of the amino groups on the PET film surface were found at  $3356\text{ cm}^{-1}$  (Figure 4a, PETN), which were assigned to the stretching vibration of the  $-\text{NH}_2$  and  $-\text{OH}$  groups, as well as the corresponding bands of the ester carbonyl groups at  $1713\text{ cm}^{-1}$  and the amide carbonyl at  $1676\text{ cm}^{-1}$ . The spectra of the PETI film (Figure 4b, PETI) did not show the presence of double bonds, indicating the successful Michael addition reaction and showing an increase in the band at  $1724\text{ cm}^{-1}$ , as well as a greater amplitude of the band located at  $3356\text{ cm}^{-1}$  corresponding to the carboxylic groups from the addition of itaconic acid and the secondary amino groups formed after the reaction.

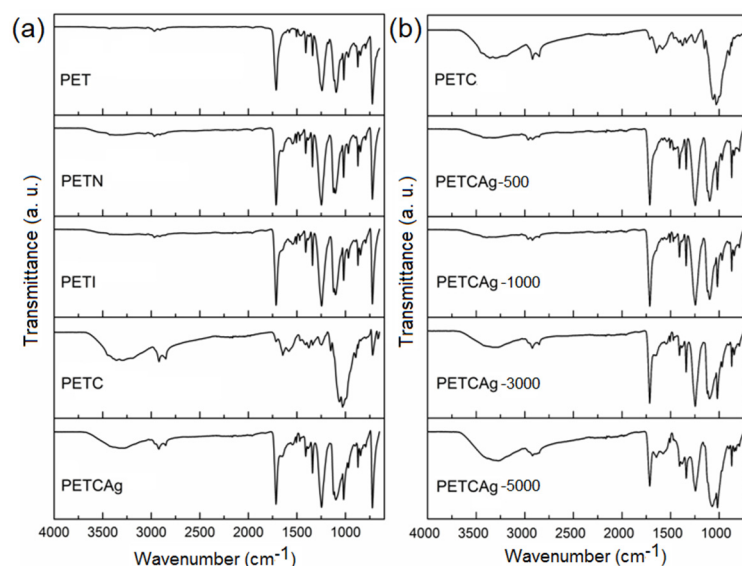


**Figure 4.** (a) FTIR-ATR spectra of PET films in the chitosan chain grafting process; (b) FTIR-ATR spectra of the PETC films loaded with silver nanoparticles in different silver nitrate concentrations.

Spectra of the PETC film indicated an adequate grafting of the chitosan polymer chains on the functionalized PET film, showing a decrease in the bands corresponding to the carbonyl groups coming from the matrix due to the coverage of grafted chitosan and showing an increase in the bands corresponding to the  $-\text{OH}$  and  $-\text{NH}_2$  groups from the chitosan chains grafted at  $3368$  and  $3299\text{ cm}^{-1}$  and amide carbonyl at  $1645\text{ cm}^{-1}$ , as well as the vibrations of the  $\text{C}-\text{H}$  bonds at  $2850\text{--}2920\text{ cm}^{-1}$  and  $\text{C}-\text{O}-\text{C}$  at  $1098\text{--}1121\text{ cm}^{-1}$ . Finally, the load of silver nanoparticles caused a broad band at  $3300\text{ cm}^{-1}$ , probably due to the interactions of the  $-\text{OH}$  and  $-\text{NH}_2$  groups with the silver nanoparticles.

This study indicated that silver nanoparticles were obtained through a reduction in silver nitrate using chitosan. The FTIR of PETCAg shows the presence of new bands at 1715 and 1250  $\text{cm}^{-1}$  due to the carboxylic and carbonyl groups confirming the oxidation of the hydroxyl groups of chitosan by the silver reduction. Likewise, the infrared spectrum shows that the carboxylic and carbonyl groups' bands increase as the silver nitrate concentration increases (Figure 4b) [31,32].

### 3.4. Thermal Analysis

The thermogravimetric analysis (Figure 5a and Table 2) shows that the films have a decomposition temperature range of 436 to 448 °C. However, after 460 °C, PETC and PETCAg films show a second decomposition range, which is attributed to the decomposition of the chitosan grafted onto the film. The amount of the residue yield obtained is shown in Table 2. DSC studies show that the melting temperature of the PET film (246 °C) was not affected by the grafting process. The PET film's glass transition ( $T_g$ ) shows an increase in the grafting process. When itaconic acid was incorporated, the  $T_g$  of PETI increased from 78.6 to 95.6 °C; the addition of chitosan raised the  $T_g$  to 100.9 °C. Loading of silver nanoparticles elevated the  $T_g$  of the PETCAg to 110.7 °C, probably due to the strong interactions of the polymer chains with the silver nanoparticles (Figure 5b) [33].

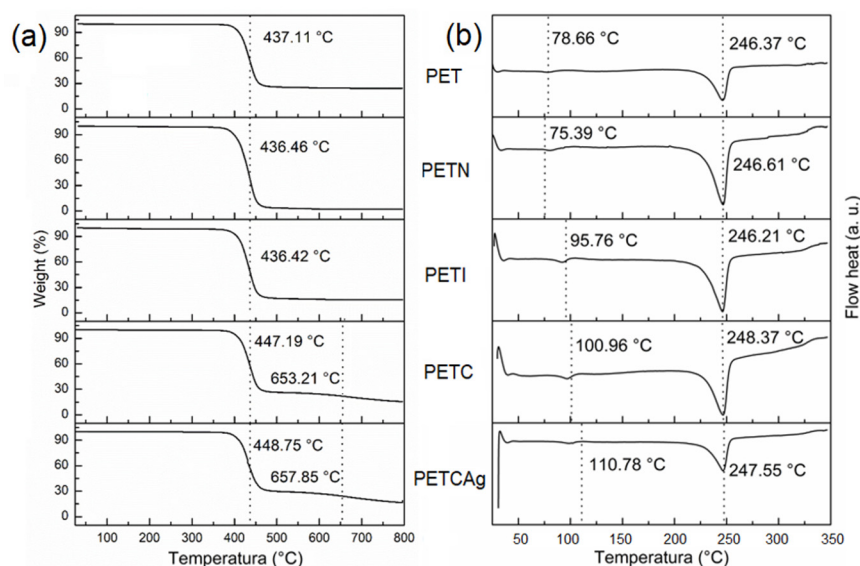


**Figure 5.** (a) TGA and (b) DSC studies under nitrogen flow on PET films obtained in the chitosan chain grafting process.

**Table 2.** Decomposition temperatures of PET films obtained in the chitosan chain grafting process.

Sample	Glass Transition Temperature (°C)	Decomposition Temperature (°C)	Residue Yield (800 °C, w.%)
PET	78.6	437.11	24.33
PETN	75.3	436.46	2.03
PETI	95.7	436.42	15.41
PETC	100.9	447.1, 653.21	7.33
PETCAg	110.7	448.75, 657.85	13.13

Silver quantification in PETC films was carried out by residual weight at 800 °C. PETC films not exposed to a silver nitrate solution presented carbonization with an average residue of 7.33%. Therefore, the residual weight difference of the total mass of the films incubated in the silver solutions (500, 1000, 3000, and 5000 ppm) can be attributed to the silver nanoparticles loaded on films, resulting in a residual weight difference of  $1.2 \pm 0.4$ ,  $2.1 \pm 0.6$ ,  $6.3 \pm 1.3$ , and  $7.1 \pm 1.4\%$ , respectively (Figure 6). As a result, a clear correlation

was observed between the amount of silver nanoparticles and the concentration of silver nitrate used in the reaction medium [34].

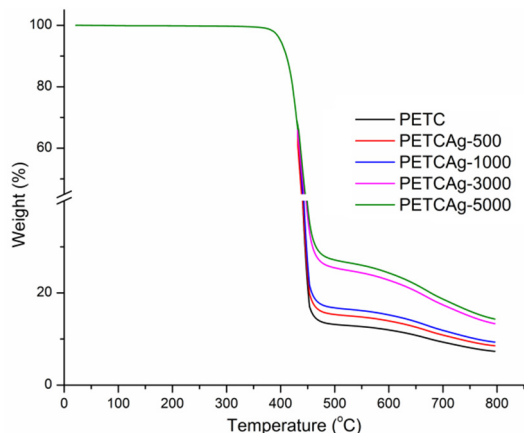


Figure 6. Silver quantification on PETC-Ag films by TGA under nitrogen flow.

### 3.5. Study of Mechanical Properties

The mechanical properties of the films were not significantly affected when grafting the chitosan polymer chains (Table 3), indicating that these were only grafted on the surface of the material, findings which were confirmed by the SEM studies, and the differences are possibly attributed to the wear of the material in the surface modification process, increasing the deformation for the PETN and PETI films, decreasing again, and becoming very similar to the original matrix for the films of PETC, with this finding being attributed to the grafting of the chitosan polymeric chains (Figure 7).

Table 3. Mechanical properties of PET films in the grafting process.

Sample	Elastic Modulus (MPa)	Stress Rupture (MPa)
PET	1144.762 ± 216.627	122.163 ± 20.3536
PETN	990.817 ± 104.047	136.780 ± 7.45101
PETI	1247.815 ± 188.311	140.172 ± 13.7654
PETC	1188.304 ± 122.115	103.506 ± 17.6539

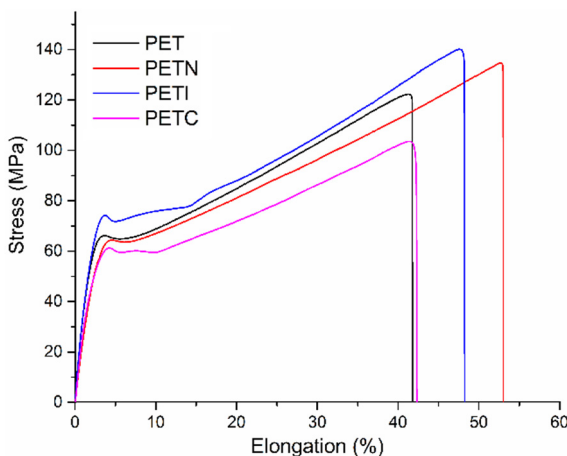
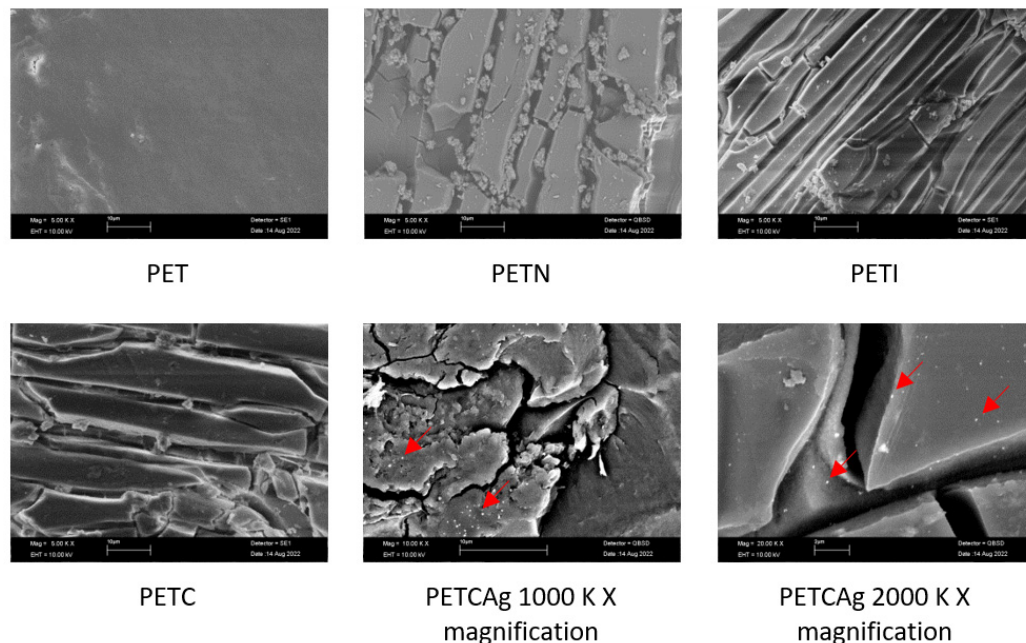


Figure 7. Tensile stress–strain graph of PET films in the process of grafting chitosan polymer chains.

### 3.6. SEM Study

SEM studies of the modified films showed relevant changes with respect to the PET films (Figure 8). The magnification showed that the film modification process caused the

formation of elongated structures in the form of layers across the surface. The formation of the layers and their thickness increased with the grafting process of the chitosan chains. Finally, the SEM images also showed the presence of silver nanoparticles on the formed chitosan layer with a mean size of  $130 \pm 37$  nm.



**Figure 8.** SEM images of PET films at different stages of the grafting process of chitosan polymer chains and with silver nanoparticles (marked with red arrows).

### 3.7. Cell Viability Study

Cell viability was evaluated against 3T3 fibroblasts (Figure 9). The cell viability of the films decreased by 15–25% compared to the control, showing no differences among these samples, as indicated by statistical analysis (Figures S1–S7, Tables S1–S4). The exception was the PETCAG-1000 film, for which viability was  $59 \pm 9.2\%$ . This finding indicates that the films, except for the PETC-1000 film, have good compatibility regardless of the modification and percentage of the silver loaded.

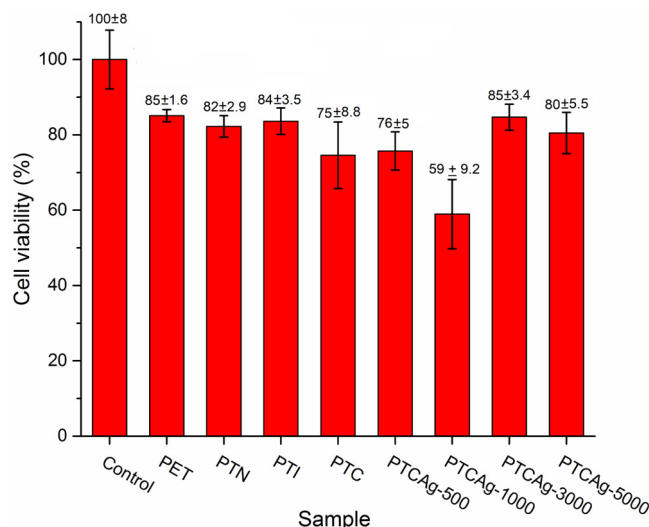


**Figure 9.** Cell viability along the grafting process (PET, PETN, PETI, and PETC) and silver-loaded PETC with different silver nanoparticles percentages (PETAg-500 ( $1.2 \pm 0.4\%$ ), PETAg-1000 ( $2.1 \pm 0.6\%$ ), PETAg-3000 ( $6.3 \pm 1.3\%$ ), and PETAg-5000 ( $7.1 \pm 1.4\%$ )).

#### 4. Conclusions

The grafting of chitosan polymer chains was successfully carried out by employing adequate surface functionalization of the PET films. The grafted chitosan allowed the nucleation and loading of silver nanoparticles with different grafted percentages (1.2–7.1% with respect to the matrix) without using other reducing agents. Silver nanoparticles with an average size of  $130 \pm 37$  nm were obtained. The films with a silver-coated surface obtained in this work are a good candidate for use as part of antimicrobial biomedical devices and disposable medical devices

**Supplementary Materials:** The following supporting information can be downloaded at: <https://www.mdpi.com/article/10.3390/polym15010125/s1>, Table S1: Analysis of Variance; Table S2: Model Summary; Table S3: Means; Table S4: Grouping Information Using the Fisher LSD Method and 95% Confidence; Figure S1: Fisher individual 95%; Figure S2: Interval plot of control PET; Figure S3: Individual value plot of control PET; Figure S4: Boxplot of control PET; Figure S5: Normal Probability Plot; Figure S6: Versus fits; Figure S7: Histogram of residual values.

**Author Contributions:** Conceptualization, G.G.F.-R. and F.L.-S.; methodology, G.G.F.-R. and E.M.; software, G.G.F.-R.; validation, E.M., R.V.-G. and E.B.; formal analysis, G.G.F.-R.; investigation, G.G.F.-R., H.M. and E.M.; resources, R.V.-G., E.M. and E.B.; data curation, H.M.; writing—original draft preparation, G.G.F.-R., F.L.-S. and E.M.; writing—review and editing, E.M.; visualization, H.M.; supervision, E.M., R.V.-G., E.B.; project administration, E.M., R.V.-G. and E.B.; funding acquisition, R.V.-G., E.M. and E.B. All authors have read and agreed to the published version of the manuscript.

**Funding:** This work was supported by the Dirección General de Asuntos del Personal Académico (DGAPA), Universidad Nacional Autónoma de México under Grant IN202320. University of Guadalajara under PROSNI 2021. Support Program for Technological Research and Innovation Projects under PAPIIT IG100220 and National Council of Science and Technology under CONACyT CF-19 No 140617. Call for basic scientific research CONACyT 2017–2018 del “Fondo Sectorial de Investigación para la educación CB2017-2018” (Grant A1-S-29789).

**Institutional Review Board Statement:** Not applicable.

**Informed Consent Statement:** Not applicable.

**Data Availability Statement:** The data presented in this study are available on request from the corresponding author.

**Acknowledgments:** Thanks to CONACyT for the postdoctoral fellowship awarded to G.G. Flores-Rojas (CVU 407270). In addition, the authors thank M.C.E. Hernández-Mecinas from the Materials Research Institute of UNAM for his technical assistance.

**Conflicts of Interest:** The authors declare no conflict of interest.

#### References

1. Berlanga, M.; Guerrero, R. Living together in biofilms: The microbial cell factory and its biotechnological implications. *Microb. Cell Factories* **2016**, *15*, 165. [[CrossRef](#)] [[PubMed](#)]
2. López-Saucedo, F.; Flores-Rojas, G.; Varca, J.; Varca, G.; Bucio, E. Antimicrobial materials and devices for biomedical applications. In *Frontiers in Clinical Drug Research: Anti-Infectives*; Rahman, A., Ed.; Bentham Science: Singapore, 2020; pp. 78–126. [[CrossRef](#)]
3. Zemljič, L.F.; Tkavc, T.; Vesel, A.; Šauperl, O. Chitosan coatings onto polyethylene terephthalate for the development of potential active packaging material. *Appl. Surf. Sci.* **2013**, *265*, 697–703. [[CrossRef](#)]
4. Mallakpour, S.; Azadi, E.; Hussain, C.M. Recent breakthroughs of antibacterial and antiviral protective polymeric materials during COVID-19 pandemic and after pandemic: Coating, packaging, and textile applications. *Curr. Opin. Colloid Interface Sci.* **2021**, *55*, 101480. [[CrossRef](#)] [[PubMed](#)]
5. Ana, P.; Bortoleto, J.; Cruz, N.; Rangel, E.; Durrant, S. Surface Properties of PET Polymer Treated by Plasma Immersion Techniques for Food Packaging. *Int. J. Nano Res.* **2018**, *1*, 33–41.
6. Sanchez-Garcia, M.D.; Gimenez, E.; Lagaron, J.M. Novel PET Nanocomposites of Interest in Food Packaging Applications and Comparative Barrier Performance with Biopolyester Nanocomposites. *J. Plast. Film Sheeting* **2007**, *23*, 133–148. [[CrossRef](#)]
7. Sulyman, M.; Haponiuk, J.; Formela, K. Utilization of Recycled Polyethylene Terephthalate (PET) in Engineering Materials: A Review. *Int. J. Environ. Sci. Dev.* **2016**, *7*, 100–108. [[CrossRef](#)]
8. Çaykara, T.; Sande, M.G.; Azoia, N.; Rodrigues, L.R.; Silva, C.J. Exploring the potential of polyethylene terephthalate in the design of antibacterial surfaces. *Med. Microbiol. Immunol.* **2020**, *209*, 363–372. [[CrossRef](#)]

9. Sun, W.; Liu, W.; Wu, Z.; Chen, H. Chemical Surface Modification of Polymeric Biomaterials for Biomedical Applications. *Macromol. Rapid Commun.* **2020**, *41*, e1900430. [[CrossRef](#)]
10. Ratner, B.; Castne, D. *Surface Modification of Polymeric Biomaterials*, 1st ed.; Springer: Boston, MA, USA, 1997. [[CrossRef](#)]
11. Zander, Z.K.; Becker, M.L. Antimicrobial and Antifouling Strategies for Polymeric Medical Devices. *ACS Macro Lett.* **2018**, *7*, 16–25. [[CrossRef](#)]
12. Bian, N.; Yang, X.; Zhang, X.; Zhang, F.; Hou, Q.; Pei, J. A complex of oxidised chitosan and silver ions grafted to cotton fibres with bacteriostatic properties. *Carbohydr. Polym.* **2021**, *262*, 117714. [[CrossRef](#)]
13. Aravamudhan, A.; Ramos, D.; Nada, A.; Kumbar, S. *Natural Polymers: Polysaccharides and Their Derivatives for Biomedical Applications*; Elsevier Inc.: Amsterdam, The Netherlands, 2014. [[CrossRef](#)]
14. Novakovic, D.; Peltonen, L.; Isomäki, A.; Fraser-Miller, S.J.; Nielsen, L.H.; Laaksonen, T.; Strachan, C.J. Surface Stabilization and Dissolution Rate Improvement of Amorphous Compacts with Thin Polymer Coatings: Can We Have It All? *Mol. Pharm.* **2020**, *17*, 1248–1260. [[CrossRef](#)] [[PubMed](#)]
15. Stoleru, E.; Munteanu, S.B.; Dumitriu, R.P.; Coroaba, A.; Drobotă, M.; Zemljic, L.F.; Pricope, G.M.; Vasile, C. Polyethylene materials with multifunctional surface properties by electro spraying chitosan/vitamin E formulation destined to biomedical and food packaging applications. *Iran. Polym. J.* **2016**, *25*, 295–307. [[CrossRef](#)]
16. Peers, S.; Montembault, A.; Ladavière, C. Chitosan hydrogels for sustained drug delivery. *J. Control. Release* **2020**, *326*, 150–163. [[CrossRef](#)] [[PubMed](#)]
17. Wang, F.; Li, J.; Tang, X.; Huang, K.; Chen, L. Polyelectrolyte three layer nanoparticles of chitosan/dextran sulfate/chitosan for dual drug delivery. *Colloids Surfaces B Biointerfaces* **2020**, *190*, 110925. [[CrossRef](#)] [[PubMed](#)]
18. Zhao, D.; Yu, S.; Sun, B.; Gao, S.; Guo, S.; Zhao, K. Biomedical Applications of Chitosan and Its Derivative Nanoparticles. *Polymers* **2018**, *10*, 462. [[CrossRef](#)] [[PubMed](#)]
19. Satitsri, S.; Muanprasat, C. Chitin and Chitosan Derivatives as Biomaterial Resources for Biological and Biomedical Applications. *Molecules* **2020**, *25*, 5961. [[CrossRef](#)] [[PubMed](#)]
20. Ji, J.; Wang, L.; Yu, H.; Chen, Y.; Zhao, Y.; Zhang, H.; Amer, W.; Sun, Y.; Huang, L.; Saleem, M. Chemical Modifications of Chitosan and Its Applications. *Polym. Technol. Eng.* **2014**, *53*, 1494–1505. [[CrossRef](#)]
21. Franconetti, A.; Carnerero, J.M.; Prado-Gotor, R.; Cabrera-Escribano, F.; Jaime, C. Chitosan as a capping agent: Insights on the stabilization of gold nanoparticles. *Carbohydr. Polym.* **2019**, *207*, 806–814. [[CrossRef](#)]
22. Phan, T.T.V.; Hoang, G.; Nguyen, V.T.; Nguyen, T.P.; Kim, H.H.; Mondal, S.; Manivasagan, P.; Moorthy, M.S.; Lee, K.D.; Junghwan, O. Chitosan as a stabilizer and size-control agent for synthesis of porous flower-shaped palladium nanoparticles and their applications on photo-based therapies. *Carbohydr. Polym.* **2019**, *205*, 340–352. [[CrossRef](#)]
23. Flores-Rojas, G.G.; López-Saucedo, F.; Vera-Graziano, R.; Mendizabal, E.; Bucio, E. Magnetic Nanoparticles for Medical Applications: Updated Review. *Macromol* **2022**, *2*, 374–390. [[CrossRef](#)]
24. Yeamsuksawat, T.; Zhao, H.; Liang, J. Characterization and antimicrobial performance of magnetic Fe<sub>3</sub>O<sub>4</sub>@Chitosan@Ag nanoparticles synthesized via suspension technique. *Mater. Today Commun.* **2021**, *28*, 102481. [[CrossRef](#)]
25. Yin, I.X.; Zhang, J.; Zhao, I.S.; Mei, M.L.; Li, Q.; Chu, C.H. The Antibacterial Mechanism of Silver Nanoparticles and Its Application in Dentistry. *Int. J. Nanomed.* **2020**, *15*, 2555–2562. [[CrossRef](#)] [[PubMed](#)]
26. El Knidri, H.; Belaabed, R.; Addaou, A.; Laajeb, A.; Lahsini, A. Extraction, chemical modification and characterization of chitin and chitosan. *Int. J. Biol. Macromol.* **2018**, *120*, 1181–1189. [[CrossRef](#)] [[PubMed](#)]
27. Sahariah, P.; Måsson, M. Antimicrobial Chitosan and Chitosan Derivatives: A Review of the Structure–Activity Relationship. *Biomacromolecules* **2017**, *18*, 3846–3868. [[CrossRef](#)] [[PubMed](#)]
28. Qian, L.; Zheng, J.; Wang, K.; Tang, Y.; Zhang, X.; Zhang, H.; Huang, F.; Pei, Y.; Jiang, Y. Cationic core–shell nanoparticles with carmustine contained within O<sup>6</sup>-benzylguanine shell for glioma therapy. *Biomaterials* **2013**, *34*, 8968–8978. [[CrossRef](#)] [[PubMed](#)]
29. Stephen, Z.R.; Kievit, F.M.; Veiseh, O.; Chiarelli, P.A.; Fang, C.; Wang, K.; Hatzinger, S.J.; Ellenbogen, R.G.; Silber, J.R.; Zhang, M. Redox-Responsive Magnetic Nanoparticle for Targeted Convection-Enhanced Delivery of O<sup>6</sup>-Benzylguanine to Brain Tumors. *ACS Nano* **2014**, *8*, 10383–10395. [[CrossRef](#)] [[PubMed](#)]
30. Veiseh, O.; Sun, C.; Gunn, J.; Kohler, N.; Gabikian, P.; Lee, D.; Bhattarai, N.; Ellenbogen, R.; Sze, R.; Hallahan, A.; et al. Optical and MRI Multifunctional Nanoprobe for Targeting Gliomas. *Nano Lett.* **2005**, *5*, 1003–1008. [[CrossRef](#)]
31. Tran, H.; Chiang, K.; Scott, J.; Amal, R. Understanding selective enhancement by silver during photocatalytic oxidation. *Photochem. Photobiol. Sci.* **2005**, *4*, 565–567. [[CrossRef](#)]
32. Wang, X.; Cheng, F.; Gao, J.; Wang, L. Antibacterial wound dressing from chitosan/polyethylene oxide nanofibers mats embedded with silver nanoparticles. *J. Biomater. Appl.* **2015**, *29*, 1086–1095. [[CrossRef](#)]
33. Vázquez, E.; Duarte, L.; López-Saucedo, F.; Flores-Rojas, G.; Bucio, E. Cellulose-based antimicrobial materials. In *Advanced Antimicrobial Materials and Applications*; Inamuddin, Ahamed, M.I., Prasad, R., Eds.; Springer: Singapore, 2021; pp. 61–85. [[CrossRef](#)]
34. López-Saucedo, F.; Flores-Rojas, G.G.; López-Saucedo, J.; Magariños, B.; Alvarez-Lorenzo, C.; Concheiro, A.; Bucio, E. Antimicrobial silver-loaded polypropylene sutures modified by radiation-grafting. *Eur. Polym. J.* **2018**, *100*, 290–297. [[CrossRef](#)]

**Disclaimer/Publisher’s Note:** The statements, opinions and data contained in all publications are solely those of the individual author(s) and contributor(s) and not of MDPI and/or the editor(s). MDPI and/or the editor(s) disclaim responsibility for any injury to people or property resulting from any ideas, methods, instructions or products referred to in the content.